The Journal of Engineering

The 14th IET International Conference on AC and DC Power Transmission (ACDC 2018)

IET Journals
The Institution of Engineering and Technology

Improved control strategy of TFAPF in active distribution networks

eISSN 2051-3305
Received on 29th August 2018
Accepted on 19th September 2018
E-First on 21st January 2019
doi: 10.1049/joe.2018.8796
www.ietdl.org

Liu Yizhao[1] ✉, Liu Huanming[1], Zhang Guangwei[1], Lei Da[1], Wang Jinhao[1], Chang Xiao[1]

[1]Electric Power Research Institute, State Grid Shanxi Electric Power Company, Taiyuan, People's Republic of China

✉ *E-mail: feixiang168899@163.com*

Abstract: In order to solve the deterioration of power quality caused by power electronic devices in active distribution networks, it is necessary to improve the three-phase four-wire active power filters (TFAPF) control strategy. This study adopts the non-harmonic detection and proposes an improved control strategy of TFAPF based on the multi-model principle. Firstly, the mathematical model of TFAPF in the stationary coordinate system is established by replacing the network side current and the DC bus voltage directly as the state variables. Secondly, TFAPF in active distribution networks requires the power fluctuation and fast dynamic response, the proposed control strategy of TFAPF in the stationary coordinate system is applied, namely proportional integral, vector resonant and repetitive control composite controller as the current loop controller of TFAPF with a fast dynamic response, high accuracy and small amount of calculation, provide guarantee for the power quality in active distribution networks. Finally, the feasibility of the proposed control strategy is verified by simulation.

1 Introduction

Currently, the active distribution network due to the access of distributed generation has the problems of power factor reduction, unbalance, harmonic pollution and so on, which seriously endanger the safe and stable operation of the active distribution network [1, 2]. Therefore, it is necessary to adopt a positive and effective scheme to solve the problem of active distribution network with distributed generation, three-phase four-wire active power filters (TFAPF) arises at the historic moment.

Typical control strategies of TFAPF include hysteresis control [3], proportional integral (PI) [4], proportional resonant (PR) control [5], many scholars have proposed fuzzy control [6], synovial variable control [7], adaptive control [8, 9], and so on. However, due to the difficulty of design, the poor control effect and the large computation, its application is limited. Compared with the above-mentioned control methods, the repetitive control (RC) based on the internal model principle has the ability to effectively track periodic signals. Also, the PR control can eliminate the steady-state error of the AC signal with a particular frequency, it has the advantages of simple calculation, high reliability, and good steady state precision, and has been widely used [10, 11].

In order to improve the dynamic response speed and stable control accuracy of TFAPF, this study proposes an improved control strategy based on the principle of multiple models. Firstly, a mathematical model of TFAPF in the stationary coordinates is established through regard the net side current, DC bus voltage as the state variable. Then the current loop controller of TFAPF is designed in the stationary coordinates, and the PI and the vector resonant (VR) control and RC are combined by the improved current loop of TFAPF. The PI control is used to enhance the stability of the TFAPF control system and improve the dynamic response rate. The static tracking control of AC and low harmonics is realised by VR, and the RC is used to realise the effective tracking control of periodic harmonic signals. The improved TFAPF has the advantages of fast dynamic response, high steady-state accuracy and a small amount of calculation. It can effectively solve the power quality problem of the active distribution network with distributed generation. The feasibility of the proposed control strategy is verified by simulation.

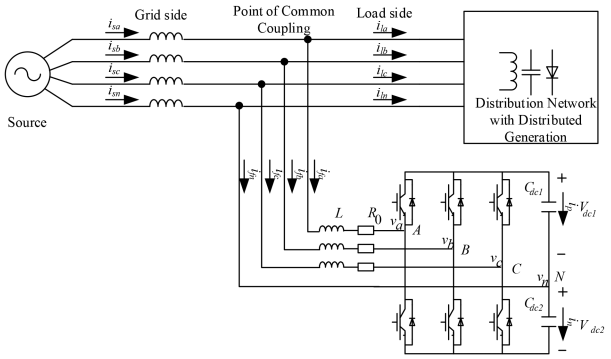

Fig. 1 *Main circuit structure of TFAPF*

2 Mathematical model of the TFAPF

As shown in Fig. 1 for the three-phase three-leg inverter with the breakdown of the capacitor as the main circuit of the TFAPF, it is capable of the active distribution network power quality problems to achieve full compensation, such as single-phase, three-phase, balanced, unbalanced, linear, non-linear and so on.

Assuming that the direction of current flowing into TFAPF is positive, then i_{si}, i_{li}, and i_{fi} are network side currents, load currents and TFAPF compensation currents, respectively. The DC bus voltage and currents of TFAPF are expressed as v_{dc} and i_p. L is the connection reactor of the TFAPF, and R_0 is the equivalent resistance considering the reactance of connection reactor, the loss of switching device and the dead time effect of the inverter. The phase voltage of v_{an}, v_{bn}, and v_{cn} is the inverter outlet. The duty cycle of d_{an}, d_{bn}, d_{cn} is the a, b, c phase bridge arm duty ratio, respectively. Equation (1) shows the mathematical model of TFAPF in the stationary coordinates. It is obtained by Kirchoff's Voltage Law and Kirchoff's Current Law theorem, combined with $i_{si} = i_{li} + i_{fi}$, through variable replacement, with grid side current, DC bus voltage as the state variable. The control variable of TFAPF in the stationary coordinates is still the AC signal, and the traditional PI control cannot achieve zero steady-state error tracking control, so it needs to adopt other advanced control algorithms

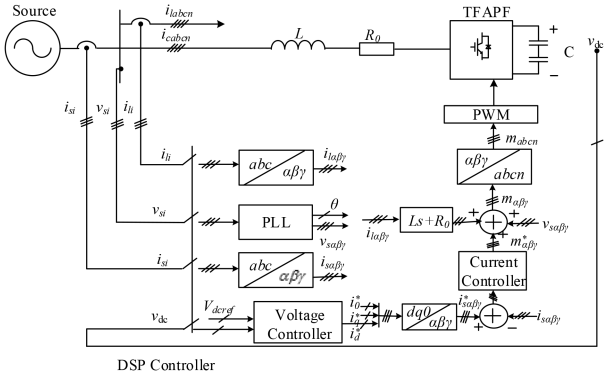

Fig. 2 *Control block diagram of TFAPF*

$$L\begin{bmatrix}\frac{\mathrm{d}i_{s\alpha}}{\mathrm{d}t}\\ \frac{\mathrm{d}i_{s\beta}}{\mathrm{d}t}\\ \frac{\mathrm{d}i_{s\gamma}}{\mathrm{d}t}\end{bmatrix}=\begin{bmatrix}e_\alpha\\ e_\beta\\ e_\gamma\end{bmatrix}-\begin{bmatrix}d_\alpha\\ d_\beta\\ d_\gamma\end{bmatrix}v_{\mathrm{dc}}-\begin{bmatrix}i_{s\alpha}\\ i_{s\beta}\\ i_{s\gamma}\end{bmatrix}R_0 +L\begin{bmatrix}\frac{\mathrm{d}i_{l\alpha}}{\mathrm{d}t}\\ \frac{\mathrm{d}i_{l\beta}}{\mathrm{d}t}\\ \frac{\mathrm{d}i_{l\gamma}}{\mathrm{d}t}\end{bmatrix}+\begin{bmatrix}i_{l\alpha}\\ i_{l\beta}\\ i_{l\gamma}\end{bmatrix}R_0+\begin{bmatrix}0\\ 0\\ \frac{v_{dc2}}{3}\end{bmatrix}, \tag{1}$$

$$C\frac{\mathrm{d}v_{\mathrm{dc}}}{\mathrm{d}t}=3d_\alpha i_{s\alpha}+3d_\beta i_{s\beta}+\frac{2}{3}d_\gamma i_{s\gamma}-\left(3d_\alpha i_{l\alpha}+3d_\beta i_{l\beta}+\frac{2}{3}d_\gamma i_{l\gamma}\right)$$

3 Improved control strategy of TFAPF

3.1 Control principle of TFAPF

As shown in Fig. 2 for the control diagram of TFAPF, it is similar to the active power filter with no harmonic detection control algorithm. It is a double closed loop cascade control system composed of a voltage outer loop and current inner loop. According to the principle of conservation of energy, by directly measuring the supply current of i_{si} and the DC bus voltage of v_{dc}, and after the operation is processed, the TFAPF outputs the compensation current needed by the distribution network. The control strategy does not need harmonic detection link and effectively improves the compensation performance and anti-interference ability of TFAPF.

The voltage outer loop adopts PI control with limiting characteristic, and the output i_{sd}* represents the total active power of the equivalent load. Considering the complete compensation of equivalent load, the q-axis current reference value i_{sq}* is set to 0, i.e. the total reactive power absorbed by the load and the TFAPF from the system side is 0; the current reference value of 0-axis i_{s0}* is set to 0, which is equivalent to the three-phase symmetrical balance of the equivalent load after TFAPF compensation. The reference current of i_{sd}*, i_{sq}*, i_{s0}* after inverse of Park's transformation coordinate transformation namely $T_{dq0/\alpha\beta\gamma}$ is the current reference value $i_{s\alpha\beta\gamma}$*. In the same way, the i_{si} ($i = a, b, c$) is transformed by CLARK transform namely $T_{abc/\alpha\beta\gamma}$ to obtain $i_{s\alpha\beta\gamma}$. The current loop reference value of $i_{s\alpha\beta\gamma}$* and network side current $i_{s\alpha\beta\gamma}$ is compared with the current controller processing producing a modulated signal $m_{\alpha\beta\gamma}$*.Taking into account the abrupt change of load and the fluctuation of grid voltage, the requirement of TFAPF dynamic response speed is considered. The modulated signal $m_{\alpha\beta\gamma}$ is obtained after the load current $i_{l\alpha\beta\gamma}$ and grid voltage $e_{\alpha\beta\gamma}$ is treated as feed forward. The $m_{\alpha\beta\gamma}$ is transformed into m_{abc} modulated by $T_{\alpha\beta\gamma/abc}$ to control the ABC phase bridge arm. Finally, the modulation signal $m_{abc}$is modulated by pulse-width modulation to generate the driving signal to control the turn-on and turn off of the insulated gate bipolar transistor, so that the desired output current is generated by the TFAPF.

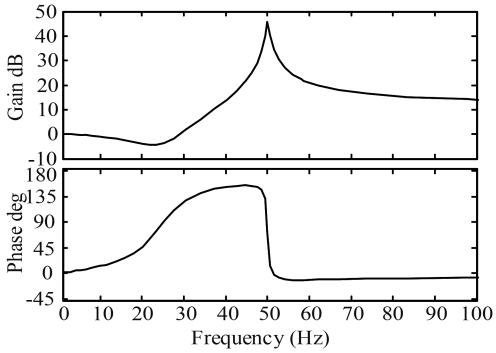

Fig. 3 *Bode diagram of VR control*

3.2 VR and RC

The VR control cannot only realise the zero steady-state error tracking control of AC signals, but also take full account of the influence of the controlled object, and has the advantages of high regulation bandwidth and good frequency selection characteristic [12–14]. The transfer function of the VR control is shown in (2), and the corresponding Bode diagram is shown in Fig. 3

$$G_{\mathrm{VR}(s)}=k_{\mathrm{P}}+k_{\mathrm{VR}}\frac{s(s+R_0/L)}{s^2+\omega_{\mathrm{c}}s+(n\omega_0)^2}, \tag{2}$$

where k_{P} and k_{VR} are scale coefficients and gain coefficients, respectively. The $n\omega_0$ is the corresponding resonant frequency point, ω_{c} is a damping factor, R_0 and L are equivalent resistance and inductor of the controlled object.

As shown in Fig. 3 it can be found that the VR control at the resonant frequency of $n\omega_0$ has high gain and can realise the fast tracking of the specific AC control signal, but the signal gain of other frequency is almost zero, does not have the ability to adjust. On the other hand, the phase lag of the VR control at the resonant point is almost 0°. Therefore, it does not affect the phase margin and the original system stability when using VR control at the resonant frequency $n\omega_0$.

Formula (3) is the transfer function of ideal RC. It adopts the internal model of the unity gain positive feedback, which makes the error converge to its repeated period, but belongs to the critical stable system, and the system stability is poor. In order to increase the stability of the system, the partial control precision is sacrificed, and the modified RC is usually used, such as (4). The internal model is modified by the attenuation coefficient Q, combined with the actual engineering experience, the Q value is taken as 0.95. Also, the correction factor $S(z)$ [15] should be designed according to the characteristics of the controlled object, as shown in Fig. 4*c* as the corresponding Bode diagram

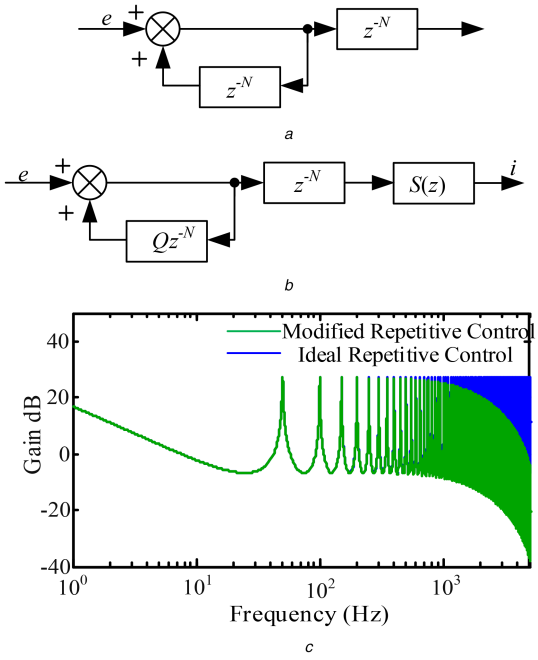

Fig. 4 *Repetitive control*
(a) Ideal RC, ***(b)*** Modified RC, ***(c)*** Bode diagram of RC

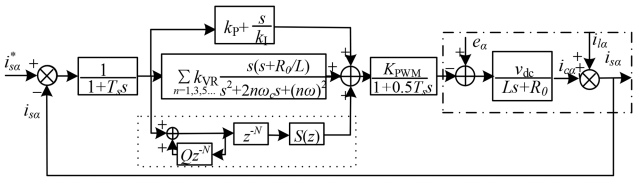

Fig. 5 *Current inner loop*

$$G_{RC}(z) = \frac{z^{-N}}{1 - z^{-N}}, \tag{3}$$

$$G^*_{RC}(z) = \frac{z^{-N}}{1 - Qz^{-N}} S(z). \tag{4}$$

In order to realise the phase and amplitude compensation of the TFAPF control system, it achieves the purpose of the unit gain and zero phase shift in the middle and low frequency, and the attenuation in the high-frequency section. The selection of the correction factor $S(z)$ parameter needs to be carried out according to the characteristics of the controlled object $GP(z)$. The correction factor $S(z)$ is composed of gain k_r, phase leading link z^k and filter link $F(z)$, such as

$$S(z) = k_r z^k F(z). \tag{5}$$

The k_r is used to regulate the magnitude of the compensation of repetitive controllers, combined with the TFAPF stability and control accuracy of the integrated needs, k_r value is 0.8 [15]. Also, the k value of the phase leading link z^k is 3 [15], which is used to compensate the total phase lag produced by the control object $GP(z)$ and the filter link $F(z)$, so as to improve the stability of the control system. The filter section $F(z)$ selects two-order low-pass filter [15], damping ratio is 0.707, turning frequency is 2.6 kHz, such as

$$F(s) = \frac{\omega_n^2}{s^2 + 2\xi\omega s + \omega_n^2}. \tag{6}$$

3.3 Improved control strategy of TFAPF

The current loop of TFAPF's α, β and γ axis is consistent in the stationary coordinates. Taking the α-axis as an example, the current inner loop control structure of the α-axis is shown in Fig. 5.

The mathematical model of TFAPF shows that the load current i_l and the power supply voltage e are the disturbance in the control process, which is not conducive to the design of the controller, especially for the active distribution network, such as intermittent load, voltage fluctuation and so on. In order to improve the dynamic response speed of TFAPF, the feed forward decoupling control strategy is adopted. The governing equations of v_α*, v_β* and v_γ* can be expressed as formula (7) refer to formula (1)

$$\begin{cases} v^*_\alpha = -G_C(s)(i^*_{s\alpha} - i_{s\alpha}) + e_\alpha + (Ls + R_0)i_{l\alpha}, \\ v^*_\beta = -G_C(s)(i^*_{s\beta} - i_{s\beta}) + e_\beta + (Ls + R_0)i_{l\beta}, \\ v^*_\gamma = -G_C(s)(i^*_{s\gamma} - i_{s\gamma}) + e_\gamma + (Ls + R_0)i_{l\gamma}. \end{cases} \tag{7}$$

The above analysis results show that there are mutual interference and serious phase lag in multiple VR control applications. The RC can simplify the VR control and deal with multiple harmonic, but the inherent cycle delay leads to poor dynamic response. Since the wide access of all kinds of power electronic devices, the active distribution network with distributed power leads to small inertia and requires higher dynamic response speed and steady state accuracy of TFAPF.

In view of the above analysis, it proposes to include PI, VR and RC composite control namely multiple internal models as the current loop controller of TFAPF. Also, the design of the TFAPF controller is finished in the stationary coordinates. The voltage outer loop controller adopts band limited PI control. In the current loop controller, PI control is to enhance the stability of the TFAPF control system and improve the dynamic response speed. VR control is realised in the fundamental frequency and low harmonic AC component without static error tracking control. RC is able to achieve the full compensation control objective of all harmonics.

As shown in formula (8) for the open loop transfer function of the TFAPF control system, the corresponding amplitude frequency characteristics as shown in Fig. 6. Ignore the influence of load current and supply voltage perturbation, the improved current loop controller not only can effectively lower fundamental frequency of AC component compensation, but can also still maintain a high gain in the high harmonic frequency, and ultimately achieve full compensation

$$O(s) = G_C(s)\frac{K_v}{(1 + 1.5T_s s)Ls + R_0}, \tag{8}$$

where $G_C(s)$ is adopted in the current loop controller with a multiple internal model transfer function available

$$\begin{aligned} G_C(s) &= k_P + \frac{k_I}{s} + \sum_{n=1}^{m} k_{VRn}\frac{s(s + R_0/L)}{s^2 + \omega_c s + (n\omega_0)^2} \\ &+ \frac{e^{-sT_s}}{1 - Qe^{-sT_s}} S(s). \end{aligned} \tag{9}$$

For PI control, VR control and RC are discretised by the bilinear transformation method, and the discrete expressions corresponding to the Z domain are obtained

$$G_{PI(z)} = \frac{((2k_P + k_I T_s)/2) - ((2k_P - k_I T_s)/2)z^{-1}}{1 - z^{-1}}, \tag{10}$$

$$G_{VR(z)} = \frac{B_0 + B_1 z^{-1} + B_2 z^{-2}}{A_0 + A_1 z^{-1} + A_2 z^{-2}}, \tag{11}$$

where $B_0 = (4k_{VR}L + 2k_{VR}R_0T_s)/L$, $B_1 = -8k_{VR}$, $B_2 = (4k_{VR}L - 2k_{VR}RT_s)/L$, $A_0 = 4 + 2\omega_c T_s + (n\omega_0 T_s)^2$, $A_1 = -\left(8 + 2(n\omega_0)^2 T_s\right)$, $A_2 = 4 - 2\omega_c T_s + (n\omega_0 T_s)^2$

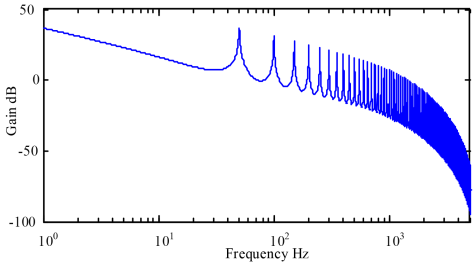

Fig. 6 *Open-loop bode plot*

Table 1 Parameters of experiment

Parameters	Value	Units
connection mode	three-phase four-wire	—
phase voltage of AC	110	V
voltage of DC	400	V
connection inductance *L*	1.2	Mh
equivalent resistance	0.1	Ω
capacitor of DC side	10,000	Uf
sampling frequency	12.8	kHz
switching frequency	12.8	kHz
load	non-linear	—

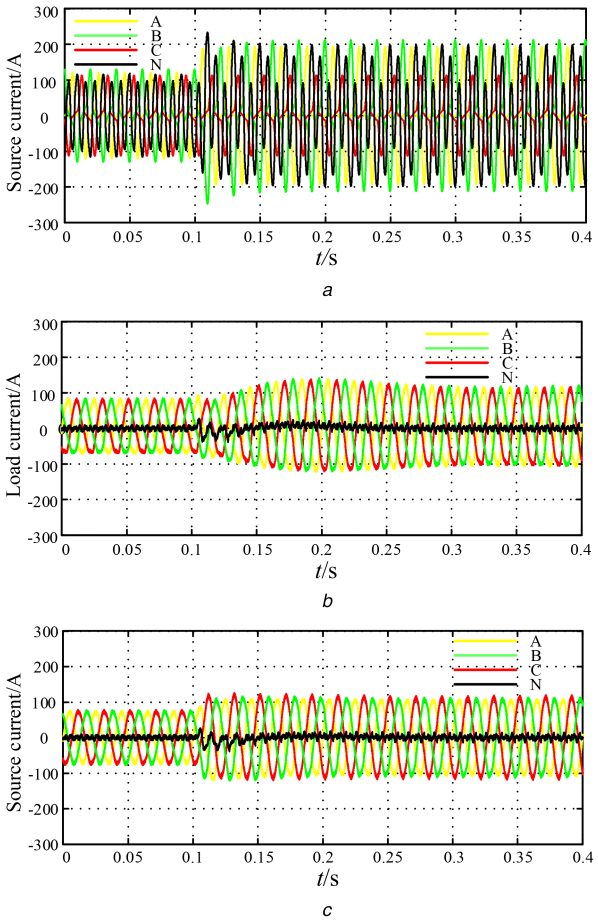

Fig. 7 *Compensation effect of TFAPF*

(a) Load current; ***(b)*** Source current by traditional control compensation; ***(c)*** Source current by improved control compensation

$$G_{\mathrm{RC}(z)} = S(z)\frac{z^{-N}}{1 - Qz^{-N}}, \tag{12}$$

where $Q = 0.95$, $N = 256$, and $S(z) = 0.8z^3((0.1282z^{-2} + 0.2565z^{-1} + 0.1282)/(z^{-2} + 0.8079z^{-1}. + 0.3208))$

4 Simulation results

In this section, the improved TFAPF control strategy based on the principle of multiple models is verified, and the TFAPF simulation model is built. The specifications of TFAPF are listed in Table 1.

As shown in Fig. 7, the steady-state compensation effect of the TFAPF is shown, at the time of $t = 0.1$ s, the effective value of the load current is 57.12, 65.09, and 54.73 A, and the mutation is 92.22, 111.1, and 54.73 A, and the corresponding total harmonic distortion (THD) is 59.03, 56.26, 46.83 and 55.07, 56.26, 46.42%, respectively; the traditional proportional RC of TFAPF for three-phase unbalance compensation of non-linear load, can effectively reduce the harmonic content and unbalance, the effective value of the source current after compensation is change from 51.6, 51.65, 51.6 A to 76.95 76.85, 76.62 A, THD content by 14.26, 14.21, 14.04, 12.11, 12.02 and 12.02% for the gradual decrease. However, by using this improved TFAPF compensation control strategy, the realisation of the source current sinusoidal three-phase balanced standard after the compensation of the effective value of 50.71, 51.15, 51.23 A to 75.95 75.01, 77.98 A, THD 3.77, 3.75, 3.84% content by 3.64, 3.95, 4.14% gradient have to meet the national standard limit of 5%, power quality has been significantly improved, as shown in Table 2.

At the same time it can be found in the moment load $t = 0.1$ s mutation in the process of using the traditional proportional RC TFAPF in the $t = 2.5$ s moments before entering the steady process, but by using this improved TFAPF transition process control strategy requires only two cycles or 40 ms will enter the steady compensation, dynamic response speed.

5 Conclusions

The particularity of power quality problems, such as voltage fluctuation, low power factor, high harmonic content, and unbalanced power supply, caused by wide access to power electronic devices in the active distribution network. This study proposes an improved control strategy of TFAPF based on the internal model principle. The non-harmonic detection algorithm is used. The grid side current and DC bus voltage are chosen as the state variable of TFAPF. Also, its mathematical model is set up in the stationary coordinate system.

A composite control strategy is proposed with multiple internal models in the stationary coordinates system with a fast dynamic response, high accuracy, and a small amount of calculation. Also, the PI control is used to enhance the stability of the TFAPF control system and improve the dynamic response rate. The static tracking control of AC and low harmonics is realised by vector resonance

Table 2 Current of load

Classification	Phase	Load current		Traditional control		Improved control	
		Value, A	THD, %	Value, A	THD, %	Value, A	THD, %
load 1	A	57.12	59.03	51.6	14.26	50.71	3.77
	B	65.09	56.26	51.65	14.21	51.15	3.75
	C	54.73	46.83	51.6	14.04	51.23	3.84
	N	77.71	—	4.02	—	3.8	—
load 2	A	92.22	55.07	76.85	12.02	75.01	3.64
	B	111.1	56.26	76.95	12.11	75.95	3.95
	C	54.73	46.42	76.62	12.02	77.98	4.14
	N	124.6	—	5.6	—	5.38	—

VR, and the RC is used to realise the effective tracking control of periodic harmonic signals.

A TFAPF of the multiple internal model compound control strategy is realised and verified by simulation.

The result proved that the multiple models of the proposed composite control of TFAPF can effectively solve the power quality problems which exists widely in active distributed networks, such as harmonic pollution, low power factor and unbalance. It is of great significance to ensure the clean, efficient and high-quality power supply of active distribution network.

6 References

[1] Shen, X., Cao, M.: 'Research on the influence of distributed power grid for distribution work', *Trans. China Electrotech. Soc.*, 2015, **30**, (S1), pp. 346–351

[2] Fu, X., Chen, H., Liu, G.*, et al.*: 'Power quality comprehensive evaluation method for distributed generation', *Proc. CSEE*, 2014, **34**, (25), pp. 4270–4276

[3] Le, J., Jiang, Q., Han, Y.: 'The analysis of hysteresis current control strategy of three-phase four-wire APF based on the unified mathematic model', *Proc. CSEE*, 2007, **27**, (10), pp. 85–91

[4] Tang, J., Luo, A., Ou, J.*, et al.*: 'Voltage control strategy of D-STATCOM based on fuzzy-PI controller', *Trans. China Electrotech. Soc.*, 2008, **23**, (13), pp. 120–126

[5] Zhang, Y., Chang, L., Yang, X.: 'Parameters setting on independent phase resonant control of STATCOM under higher voltage and RTDS simulation experiment', *Power Syst. Prot. Control*, 2016, **44**, (15), pp. 27–32

[6] Quoc-Nam, T., Hong-Hee, L.: 'An advanced current control strategy for three-phase shunt active power filters', *IEEE Trans. Ind. Electron.*, 2013, **60**, (12), pp. 5400–5410

[7] Zhu, H., Luo, L: 'A comprehensive variable structure control for HVDC power transmission and generator excitation', *Power Syst. Technol.*, 2012, **36**, (3), pp. 223–227

[8] Fu, X., Wang, J., JI, Y*, et al.*: 'Adaptive deadbeat control in stationary reference frame for D-STATCOM', *Autom. Electr. Power Syst.*, 2007, **31**, (8), pp. 41–45 + 79

[9] Bhim, S., Jitendra, S.: 'An implementation of an adaptive control algorithm for a three-phase shunt active filter', *IEEE Trans. Ind. Electron.*, 2009, **56**, (8), pp. 2811–2820

[10] Jiang, D., Zhang, Z.: 'Control scheme of three-phase H-bridge cascaded STATCOM', *High Volt. Eng.*, 2011, **37**, (8), pp. 2024–2031

[11] Zhao, X., Shi, L., Chen, L.: 'A new current control strategy of cascaded STATCOM with composite control', *Power Syst. Prot. Control*, 2015, **43**, (17), pp. 98–106

[12] Cristian, L., Lucian, A., Ion, B.*, et al.*: 'Frequency response analysis of current controllers for selective harmonic compensation in active power filters', *IEEE Trans. Ind. Electron.*, 2009, **56**, (2), pp. 337–347

[13] Cristian, L., Lucian, A., Ion, B.*, et al.*: 'High performance current controller for selective harmonic compensation in active power filters', *IEEE Trans. Power Electron.*, 2007, **22**, (5), pp. 1826–1835

[14] Xu, M., Xu, D., Lin, P.: 'Understanding repetitive control and resonant control'. 3rd IEEE Int. Symp. on Power Electronics for Distributed Generation Systems (PEDG), 2012, pp. 621–627

[15] Kai, Z., Yong, K., Jian, X.*, et al.*: 'Direct repetitive control of SPWM inverter for UPS purpose', *IEEE Trans. Power Electron.*, 2003, **18**, (3), pp. 84–792